Supporting Information for

An Ising Iron(II) Chain Exhibits Large Finite-Size Energy Barrier and "Hard" Magnetic Behaviour

Yi-Fei Deng,[a] Tian Han,*[a] Wei Xue,[b] Naoaki Hayashi,[c,d] Hiroshi Kageyama[e,f] and Yan-Zhen Zheng*[a]

[a] Frontier Institute of Science and Technology (FIST) and School of Science, State Key Laboratory for Mechanical Behavior of Materials, Xi'an Jiaotong University, Xi'an 710054, China.

[b] School of Chemistry & Chemical Engineering, Sun Yat-Sen University, Guangzhou 510275, China.

[c] Research Institute for Production Development, Shimogamo, Sakyo, Kyoto 606-0805, Japan.

[d] Institute for Integrated Cell-Material Sciences, Kyoto University, Sakyo, Kyoto 606-8501, Japan.

[e] Department of Energy and Hydrocarbon Chemistry, Graduate School of Engineering, Kyoto University, Nishikyo-ku, Kyoto 615-8510, Japan.

[f] CREST, Japan Science and Technology Agency (JST), Kawaguchi, Saitama 332-0012, Japan.

Email: zheng.yanzhen@xjtu.edu.cn hantian0123@xjtu.edu.cn

Table S1. Crystal data and structure refinement for **1**.

	1
formula	$C_7H_7FeN_7O_2$
M / g mol^{-1}	277.05
Crystal system	Triclinic
space group	P-1
a, Å	6.400(2)
b, Å	8.580(3)
c, Å	10.802(4)
α, deg	106.749(5)
β, deg	104.441(4)
γ, deg	96.194(5)
V, Å^3	539.6(4)
Z	2
d_{cal}/g cm^{-3}	1.705
Temperature, K	296(2)
θ range	2.06–27.40°
completeness	0.986
Goodness-of-fit on F^2	1.046
final indices [$I > 2\sigma(I)$]	$R_1 = 0.0499$, $wR_2 = 0.1468$
R indices (all data)	$R_1 = 0.0627$, $wR_2 = 0.1551$

Table S2. Selected bond lengths (Å) and angles (º) for complex **1**.

Bonds	Å	Angles	°
Fe(1)-O(1)	2.072(3)	O(1)#1-Fe(1)-O(1)	180.000(1)
Fe(1)-N(5)	2.203(3)	O(1)#1-Fe(1)-N(5)	88.87(12)
Fe(1)-N(4)	2.204(3)	O(1)-Fe(1)-N(5)	91.13(12)
Fe(2)-O(2)	2.127(3)	N(5)-Fe(1)-N(5)#1	180.000(1)
Fe(2)-N(4)	2.187(3)	O(1)-Fe(1)-N(4)	90.30(13)
Fe(2)-N(5)	2.200(3)	N(5)-Fe(1)-N(4)	82.39(13)
O(1)-C(1)	1.247(4)	N(5)#1-Fe(1)-N(4)	97.61(13)
O(2)-C(1)	1.251(4)	O(1)-Fe(1)-N(4)#1	89.70(13)

N(1)-C(6)	1.344(5)	N(4)-Fe(1)-N(4)#1	180.000(1)
N(1)-C(4)	1.346(5)	O(2)#2-Fe(2)-O(2)	180.000(1)
N(1)-C(5)	1.478(5)	O(2)-Fe(2)-N(4)#2	87.80(12)
N(2)-N(3)	1.145(5)	O(2)-Fe(2)-N(4)	92.20(12)
N(3)-N(4)	1.210(5)	N(4)#2-Fe(2)-N(4)	180.000(1)
N(5)-N(6)	1.186(5)	O(2)-Fe(2)-N(5)	89.79(12)
N(6)-N(7)	1.152(6)	N(4)-Fe(2)-N(5)	82.84(13)
C(1)-C(2)	1.513(5)	O(2)-Fe(2)-N(5)#2	90.21(12)
C(2)-C(7)	1.387(5)	N(4)-Fe(2)-N(5)#2	97.16(13)
C(2)-C(3)	1.392(5)	N(5)-Fe(2)-N(5)#2	180.000(1)
C(3)-C(4)	1.366(6)	C(1)-O(1)-Fe(1)	130.5(2)
C(6)-C(7)	1.378(6)	C(1)-O(2)-Fe(2)	127.5(2)

Symmetry transformations used to generate equivalent atoms:
#1 -x+1,-y+1,-z+1 #2 -x,-y+1,-z+1

Table S3. The best results fitted for **1** under 0 Oe dc field and 1000 Oe dc field by a generalized Debye model.

0 Oe			1000 Oe		
T / K	τ	α	T / K	τ	α
6.40	2.60×10^{-2}	0.44	6.39	1.28×10^{-1}	0.56
6.88	6.85×10^{-3}	0.42	6.87	3.69×10^{-2}	0.55
7.30	2.64×10^{-3}	0.40	7.36	9.78×10^{-3}	0.54
7.83	7.69×10^{-4}	0.40	7.77	2.69×10^{-3}	0.52
8.33	3.18×10^{-4}	0.39	8.33	8.36×10^{-4}	0.50
8.76	1.42×10^{-4}	0.38	8.81	2.89×10^{-4}	0.48
9.31	6.75×10^{-5}	0.37	9.30	9.97×10^{-5}	0.46
9.75	3.35×10^{-5}	0.35	9.72	5.41×10^{-5}	0.44
10.71	8.90×10^{-6}	0.34	10.76	1.05×10^{-5}	0.44

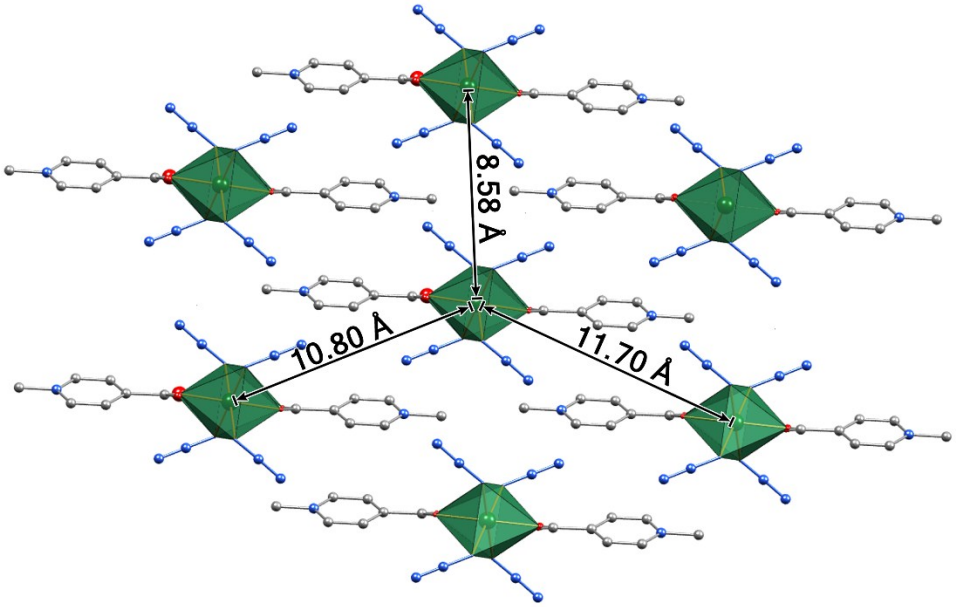

Figure S1. The packing diagram of **1** showing the interchain distances. Colour codes: green = Fe, red = O, grey = C, light blue = N.

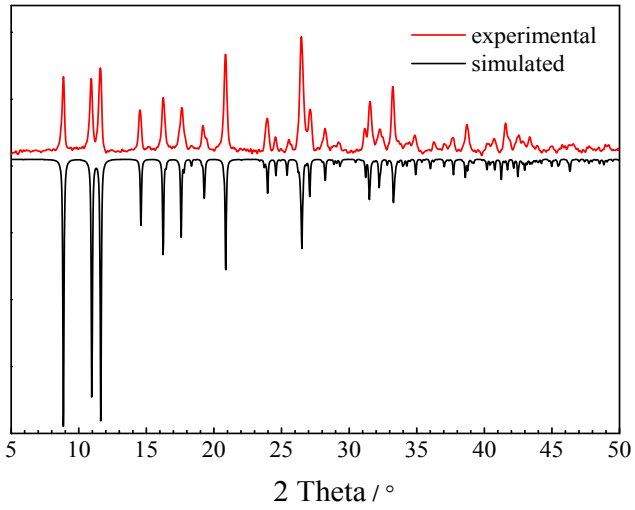

Figure S2. The experimental and calculated powder XRD patterns of **1.**

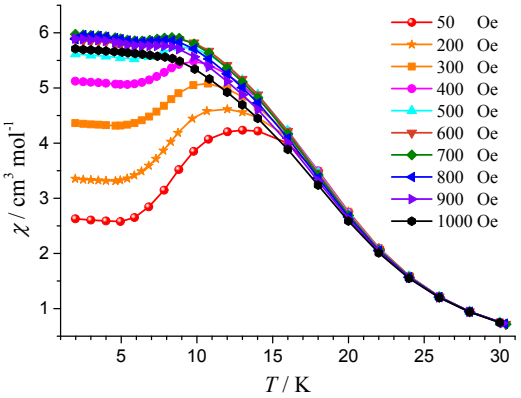

Figure S3. Plots of χ_M vs T under an applied field of 50-1000 Oe. Solid lines are guides for the eyes.

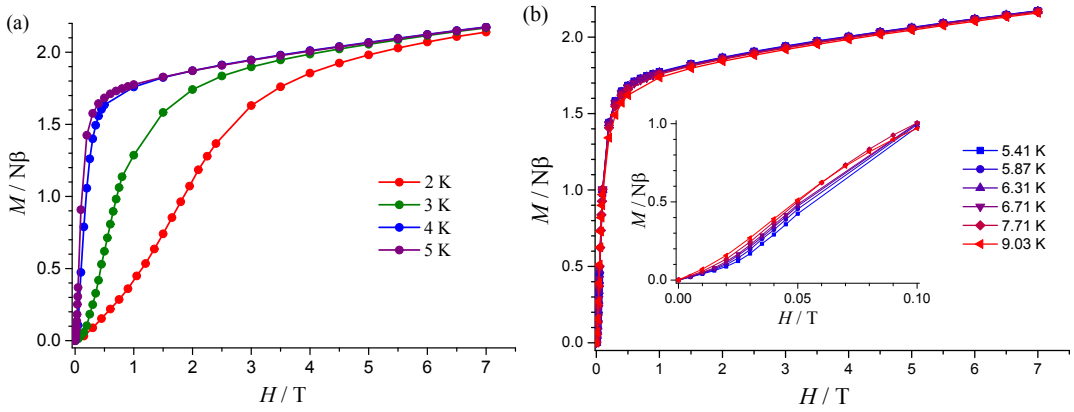

Figure S4. Field dependence of the magnetization (*M*) for **1** below 5 K (a) and between 5.41 and 9.03 K (b). Insert: the enlarged *M* versus *H* plots for **1** between 5.41 and 9.03 K. Solid lines are guides for the eyes.

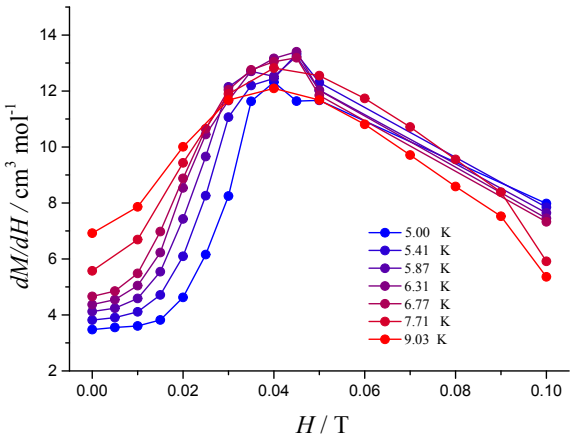

Figure S5. First field derivative of the magnetization as a function of the applied dc-field for **1** between 5.00 and 9.03 K. These plots are obtained from the data shown in Figure S4. Solid lines are guides for the eyes.

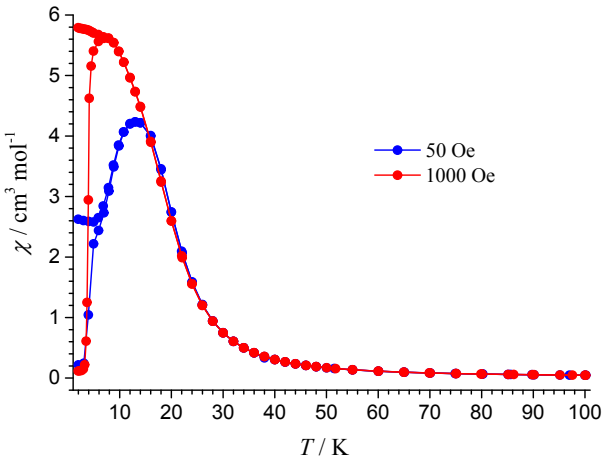

Figure S6. ZFC and FC magnetization versus temperature curves of **1** measured with applied fields of 50 and 1000 Oe. Solid lines are guides for the eyes.

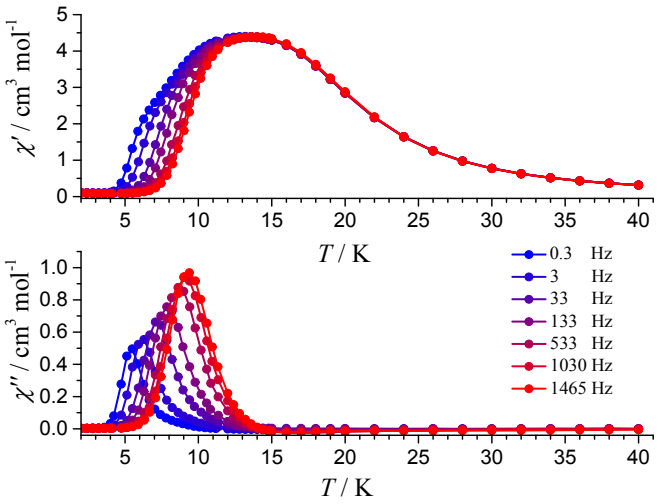

Figure S7. Temperature dependence of the in-phase (χ') and out-of-phase (χ'') parts of the ac susceptibility for **1** under zero dc field. Solid lines are guides for the eyes.

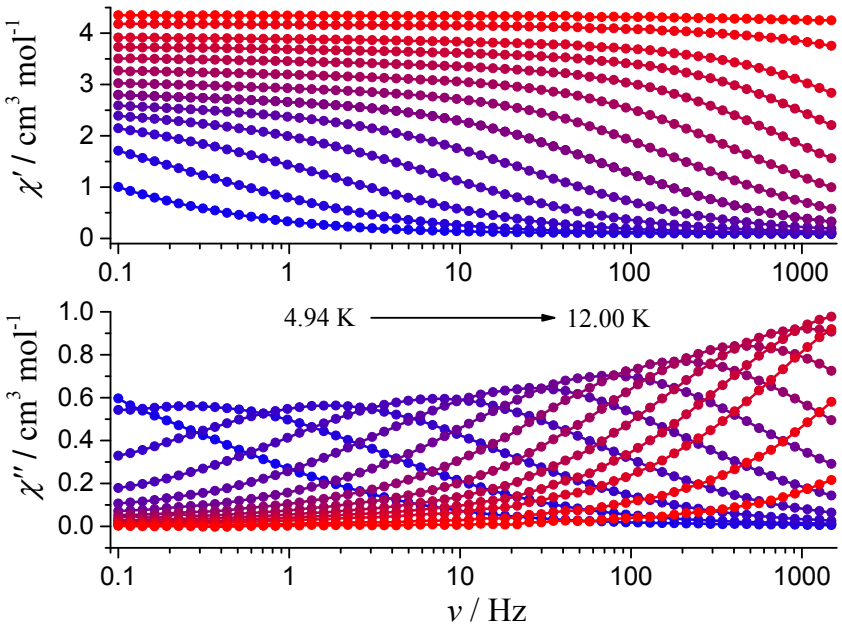

Figure S8. Frequency dependence of the in-phase χ' (top) and out-of-phase χ'' (bottom) parts of the ac susceptibility for **1** under zero dc field. Solid lines are guides for the eyes.

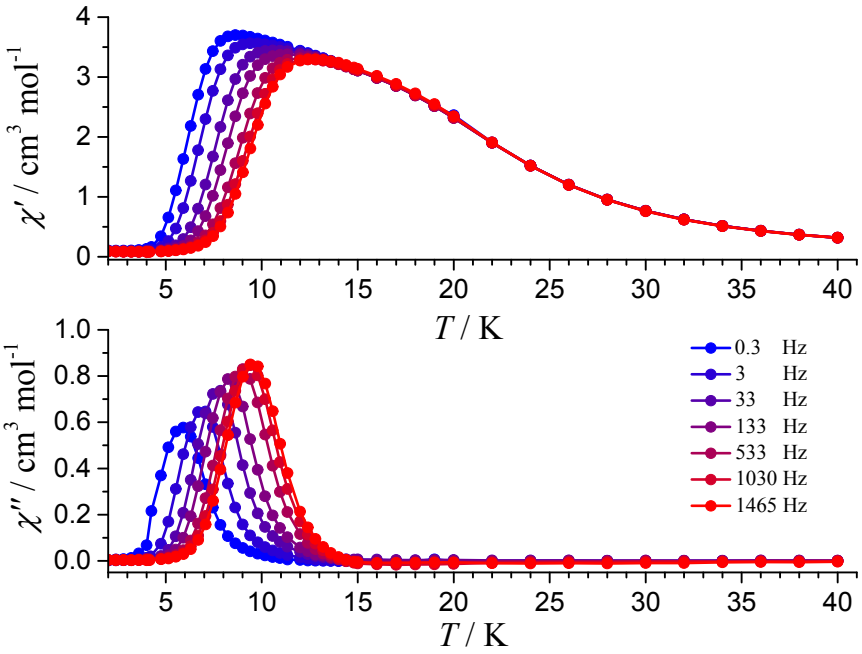

Figure S9. Temperature dependence of the in-phase (χ') and out-of-phase (χ'') parts of the ac susceptibility for **1** under 1000 Oe dc field. Solid lines are guides for the eyes.

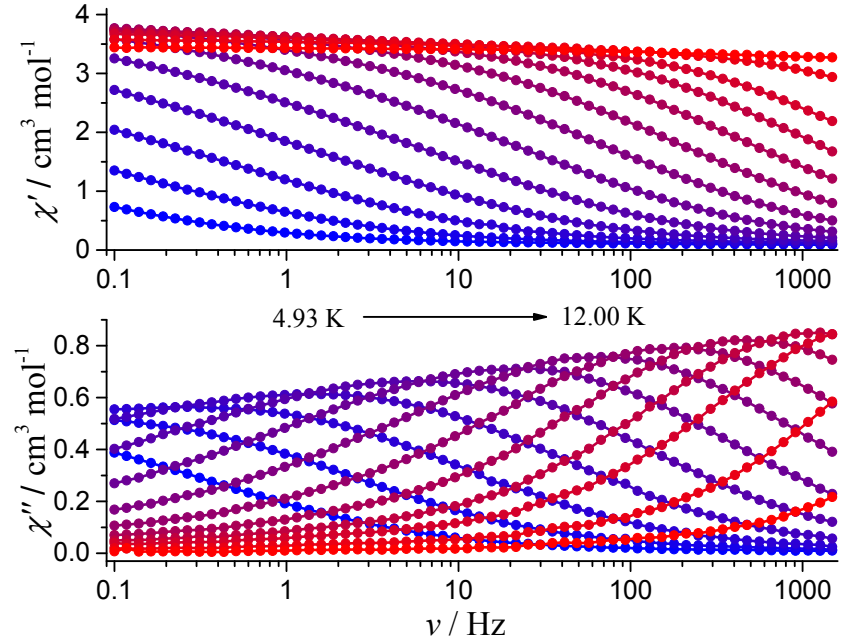

Figure S10. Frequency dependence of the in-phase χ' (top) and out-of-phase χ'' (bottom) parts of the ac susceptibility for **1** under 1000 Oe dc field. Solid lines are guides for the eyes.

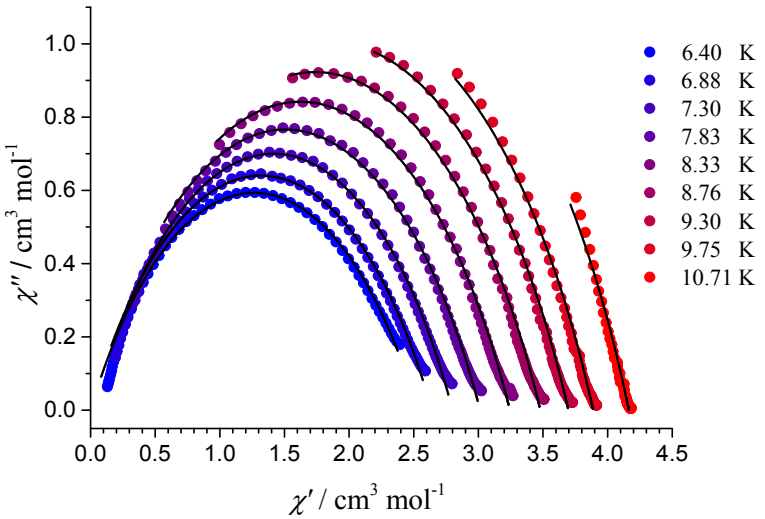

Figure S11. Cole-Cole plots of **1** under zero dc field. Black lines represent best fits to a generalized Debye Model.

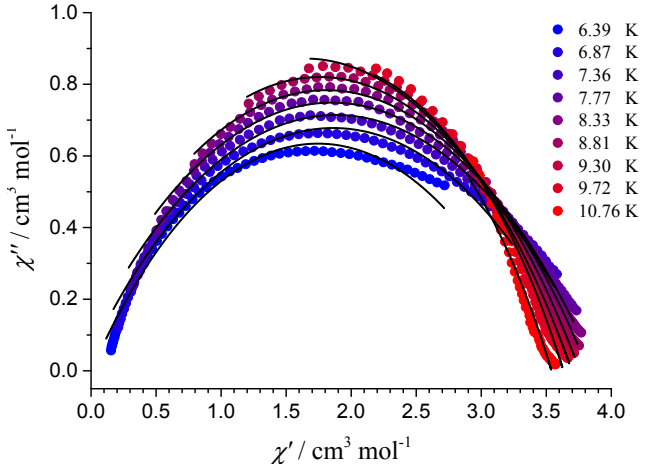

Figure S12. Cole-Cole plots of **1** under 1000 Oe dc field. Black lines represent best fits to a generalized Debye Model.

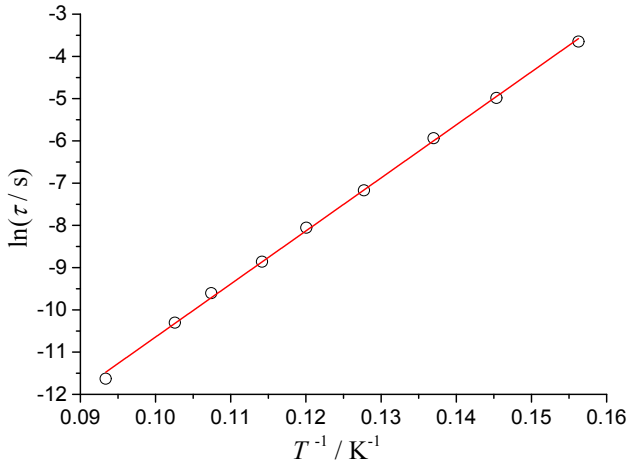

Figure S13. Magnetization relaxation time (τ) versus T^{-1} plot for **1** under zero dc field. The solid line represents the best fit to Arrhenius Law.

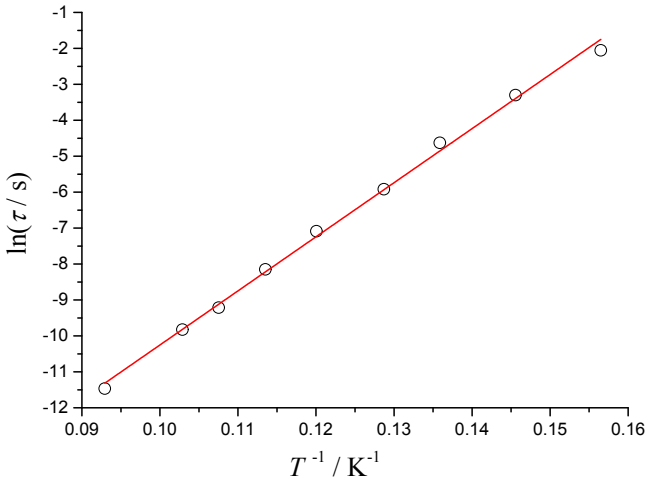

Figure S14. Magnetization relaxation time (τ) versus T^{-1} plot for 1 under 1000 Oe dc field. The solid line represents the best fit to Arrhenius Law.

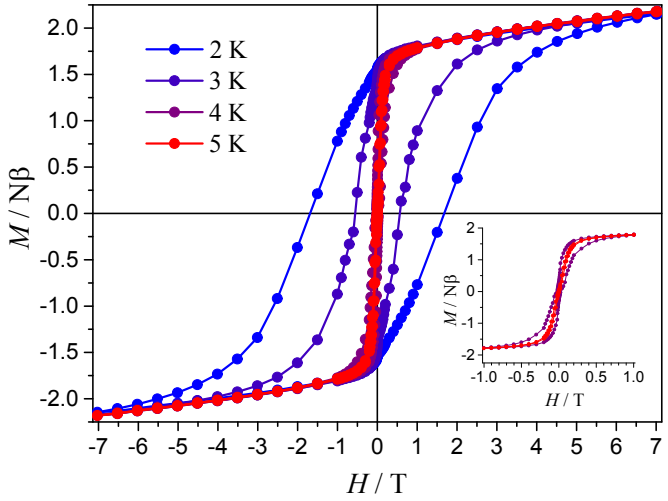

Figure S15. Hysteresis loops of **1** measured between 2 and 5 K with a field sweep rate of 14 Oe/s. The lines are guides for the eyes. Insert: Enlarged hysteresis loops of **1** at 4 and 5 K.

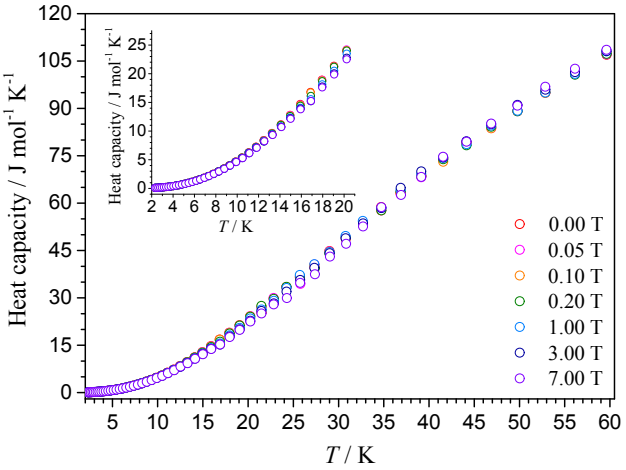

Figure S16. The heat-capacity plots of **1** under various fields in the temperature range of 2-60 K. Inset: The heat-capacity plots of **1** in the temperature range of 2-21 K.